



Synthesis gas fermentation at high cell density: How pH and hydrogen partial pressure affect productivity and product ratio in continuous fermentation

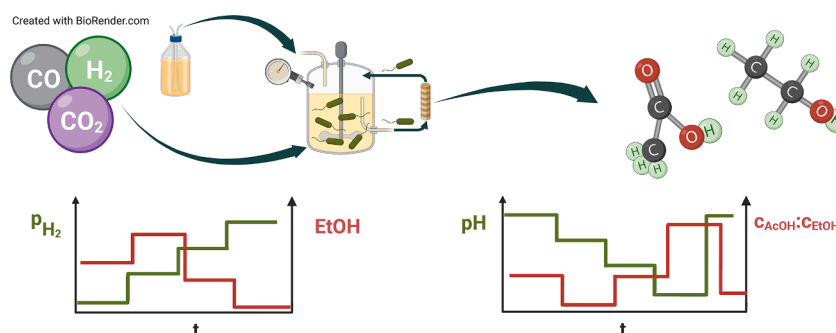
Lukas Perret^{a,*}, Nikolaos Boukis^a, Jörg Sauer^a

^a Institute of Catalysis Research and Technology, Karlsruhe Institute of Technology, Hermann-von-Helmholtz-Platz 1, Eggenstein-Leopoldshafen 76344, Baden-Württemberg, Germany

HIGHLIGHTS

- Continuously operated syngas fermentation at increased cell density and pressure.
- Highest ethanol space-time yield of $10\text{mmolL}^{-1}\text{h}^{-1}$ at $p_{\text{H}_2} = 1.52$ bar.
- $p_{\text{H}_2} = 4.45$ bar results in large decrease in cell density and hydrogen uptake.
- pH lower than 5.7 leads to increased acetic acid formation.

GRAPHICAL ABSTRACT



ARTICLE INFO

Keywords:

Continuous syngas fermentation
Hydrogen partial pressure
pH
Biomass retention
Steady-state measurements

ABSTRACT

For the first time, syngas fermentation was operated continuously with total cell retention and process pressures up to 4 barg in long-term runs of up to 3000 hours. Throughout this time, the process was stable. The measured data have shown that hydrogen uptake and ethanol space-time yield are highest at a slightly reduced pH of 5.7 compared to pH 5.9. Even lower pH values lead to higher acetic acid to ethanol product ratios, while C₂ space-time yields remain constant. Increasing the hydrogen partial pressure to 1.52 bar resulted in a significant increase in hydrogen uptake rate and ethanol formation. An ethanol space-time yield of $10\text{mmolL}^{-1}\text{h}^{-1}$ was short-term achieved, being the highest space-time yield measured to date for the wild type of *C. ljungdahliae*. Hydrogen uptake above a theoretical equilibrium concentration of $1.2\text{mmolH}_2\text{L}^{-1}$ is significantly reduced, indicating an inhibition of an enzymatic reaction.

1. Introduction

Synthesis gas fermentation can be used to convert gases such as

CO, CO₂ and H₂ to high added-value products such as ethanol, butanol or hexanol (Fernández-Blanco et al., 2023). Bacteria of the type Clostridia can be used as biocatalysts to fix carbon by using the Wood-

* Corresponding author.

E-mail address: lukas.perret@kit.edu (L. Perret).

<https://doi.org/10.1016/j.biortech.2023.129894>

Received 30 August 2023; Received in revised form 17 October 2023; Accepted 17 October 2023

Available online 20 October 2023

0960-8524/© 2023 The Author(s). Published by Elsevier Ltd. This is an open access article under the CC BY license (<http://creativecommons.org/licenses/by/4.0/>).

Ljungdahl pathway.

However, low cell densities and their associated low space–time yields, which can be up to three orders of magnitude lower compared to heterogeneous catalysis, are still major hurdles on the way to commercialization (Perret et al., 2022).

To determine the reaction engineering principles of monoculture with *C. ljungdahliae* and to understand the influence of the key process parameters on the reaction, experiments in continuous mode are a prerequisite and of essential importance. Studies in batch mode are not very useful, since product inhibition or medium limitations can occur during the course of the experiment.

Perret et al. (2023) have shown that the use of a biomass retention system can significantly increase cell density and space–time yields, while at the same time shifting product ratio towards ethanol. Younesi et al. (2005) found that they were able to increase overall productivity and ethanol space–time yield by increasing process pressure. Abubackar et al. (2018) use a two-stage reactor setup to achieve high growth at optimal pH in stage 1 and increased ethanol formation at reduced pH in stage 2.

However, detailed studies on the influence of increased partial pressure of H₂ and reduced pH on syngas fermentation at high cell densities and continuous operation are missing. Therefore, the following study answers two questions in more detail:

1. When using a biomass retention system, is it possible to increase the hydrogen uptake rate by increasing the process pressure at a constant volumetric hydrogen input, thus further increasing ethanol formation? The constant-volume hydrogen feed implies an increase in the hydrogen partial pressure in order to improve the gas–liquid mass transfer of H₂.
2. With the use of a biomass retention system and already high space–time yields of ethanol, can the product ratio be shifted even further in the direction of ethanol by lowering the pH?

With the novel experimental setup used for this study, it is possible to carry out fermentation experiments in fully continuous operating mode with pH control, a biomass retention system to increase cell density, and with pressure-stable designs to increase process pressure. With this setup, it is possible to fill the current knowledge gap on the influence of pH and H₂ partial pressure at high cell densities. These data would also provide an important basis for future studies on the co-cultivation of *C. ljungdahliae* and caproate-producing bacteria, which could be used to convert acetic acid and ethanol to higher added-value products.

2. Materials and Methods

2.1. Microorganism, cultivation and nutrient medium

For biocatalysis, *Clostridium ljungdahliae* (DSM 13528), an anaerobic, acetogenic bacterium, is used. The composition of the culture medium for pre-cultivation and process is the same as described in Perret et al. (2023). The pH of the culture medium is adjusted to the same value as in the reactor by adding KOH pellets. The culture medium is initially anaerobized by adding gaseous nitrogen in a first step and then sterilized at 121 °C for 20 min. The culture medium is then anaerobized with a sterile gas mix of 80 vol.% N₂ and 20 vol.% CO₂. For pre-cultivation, 1 g/L cysteine-HCl·H₂O is sterilely injected into the culture medium, while for the culture medium supplied in continuous operating mode 0.3 g/L is sterilely injected. The detailed procedure for anaerobic pre-cultivation in three steps at 37 °C is described in Stoll et al. (2019).

2.2. Experimental setup

In Fig. 1, the test rig for the continuous fermentation is shown. A gas and a nutrient stream are continuously fed to the reactor, which has a volume of 4 liter. To keep the pH of the fermentation broth constant, a

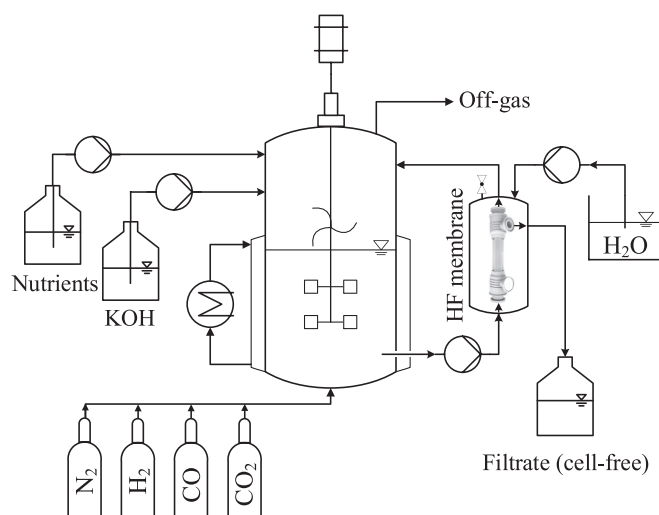


Fig. 1. Experimental setup for a continuous fermentation including cross-flow filtration with a hollow fiber (HF) membrane (reference: repligen.com) in an external circuit for biomass retention. The hollow fiber membrane is placed in a pressure-stable vessel flooded with water. The pressure in the vessel can be increased by adding water via a pump and thus adapted to the process pressure in the reactor.

base is automatically added. Furthermore, there is an external circuit of cross-flow filtration with a hollow fiber membrane for biomass retention. Bacteria are not able to leave the system, since the cross filtration module is too fine to cross (0.2 μm). This circuit is also sterilized before the start of the experiment and is not opened again during the experiment. For this study, the experimental plant of Perret et al. (2023) was extended by a pressure-stable vessel for the hollow fiber membrane. The hollow fiber membrane is placed in a pressure-stable vessel flooded with water. The pressure in the vessel can be increased by adding water via a pump and thus adapted to the process pressure in the reactor. This device allows the hollow fiber membrane for cross-flow filtration to be operated at higher pressures, since by bringing the pressure in the vessel into line with the process pressure in the reactor, the hollow fiber membrane does not experience any significant differential pressure (maximum allowed differential pressure of the membrane: 2 bar). For the detailed design of the pressure-stable construction for the hollow fiber membrane, see supplementary material. In this configuration, the hollow fiber membrane can be operated for over 3000 process hours. All other technical components in Fig. 1 are the same as in Perret et al. (2023), details, and also the procedure for sterilization, can be found there.

2.3. Process parameters

The measurement data presented in the present study were obtained during two long-term experiments:

- Experiment A was performed to study the effects of a pressure increase at a constant volumetric hydrogen feed, this experiment had a duration of 1970 h. The other gases were fed mass-constant. The process pressure was increased from atmospheric pressure conditions (0 barg) to 1 barg, 2 barg, 3 barg and finally 4 barg.
- Experiment B was used to study the effect of a pH reduction at ambient pressure conditions, the process time was 3097 h. Starting at pH 5.9, the pH was lowered to 5.7, 5.5, 5.3, and 5.1 before being raised again to 5.9. The other experimental parameters were kept constant.

Due to the constant volumetric hydrogen feed at increased pressure, the gas–liquid mass transfer coefficient $k_L a$ of hydrogen is kept constant.

The estimation of the $k_L a$ of hydrogen is calculated according to Stoll (2021):

$$k_L a_{H_2} = f_{H_2} \cdot 11.82 \cdot \left(\frac{P}{V_1}\right)^{0.26} \cdot \left(u_{G,H_2} \cdot \frac{p_0}{p_R}\right)^{0.97} \quad (1)$$

f_{H_2} with a value of 1.19 represents a conversion factor, P/V_1 is the specific energy input into the CSTR, u_{G,H_2} represents the gas velocity of hydrogen, p_0 represents the ambient pressure in bar and p_R the pressure in the reactor in bar.

Both experiments were conducted in a fully continuous operation mode with a cell retention system. For all experiments, the following parameters remain the same: the temperature in the reactor is 37 °C, the dilution rate is 0.03 h⁻¹, the liquid retention time τ is 33.3 h, and the gas residence time is between 8 min and 23 min. The composition of the substrate gas was chosen to ensure that hydrogen is present in excess for the stoichiometrically complete conversion of CO and CO₂ to ethanol. The reaction volume in the 4-liter reactor is 2.2 liters; the volume of the circuits for level detection of 269 ml and biomass retention of 126 ml do not count as part of the reaction volume. In the CSTR, the specific energy input P/V_1 by the stirrer (600 rpm) is 1.36 kW m⁻³. The volume flow in the external circuit for biomass retention is 10 L h⁻¹, resulting in a residence time of the liquid phase in this circuit of 45 s. There is no gas feeding in this external circuit. For the evaluation, measurement data from steady-state intervals were averaged. Steady-state intervals are areas where gas uptake rates and productivities stay constant without continuous increase or decrease, fluctuating around an average value with a standard deviation less than 10%. Further process parameters can be taken from Table 1 and Table 2.

2.4. Analytical methods

The composition of the exhaust gas is analyzed using a micro gas chromatograph. In addition, cell density, carbon content and product concentrations are determined by taking a liquid sample from the reactor. The detailed procedure and technical specifications of the analytical equipment are the same as for Perret et al. (2023) and have already been described in detail there.

Table 1

Experimental parameters of experiment A to study the influence of a pressure increase at a constant volumetric hydrogen input. The intervals 0 barg, 1 barg, 1 barg_(CO₂), 2 barg and 3 barg represent steady-state areas from experiment A in a fully continuous operation mode. Four different pressure levels were investigated, with the pressure-specific volumetric hydrogen input \dot{V}_{H_2}/p kept constant. In interval 1 barg_(CO₂), the amount of supplied CO₂ in the substrate gas was increased.

	0 barg	1 barg	1 barg _(CO₂)	2 barg	3 barg
p / barg	0	1	1	2	3
$\dot{V}_{G,n}$ / mL.min ⁻¹	97	157	158	216	275
H ₂ /CO/CO ₂ /N ₂ / vol. %	61/20/7/12	76/12/4/8	75/12/5/8	83/9/3/5	87/7/2/4
p_{H_2} / bar	0.61	1.52	1.5	2.49	3.48
p_{CO} / bar	0.2	0.24	0.24	0.27	0.28
p_{CO_2} / bar	0.07	0.08	0.1	0.09	0.08
$k_L a(H_2)$ / s ⁻¹ · 10 ⁻²	0.96	0.95	0.95	0.96	0.96
$\frac{\dot{V}_{H_2}}{p}$ / mL.min ⁻¹ bar ⁻¹			← 59.42 →		
pH			← 5.85 →		
duration of interval/ h	38.6	42	59.6	55	37.5
number of gas samples	155	168	235	220	150
number of liquid samples	3	4	5	3	3

Table 2

Experimental parameters of experiment B to study the influence of different pH values. The intervals pH 5.9, pH 5.7, pH 5.5 and pH 5.9 represent steady-state areas at three different pH values from experiment B in a fully continuous operation mode. At the end of the experiment, the pH value of 5.9 investigated at the beginning in interval pH 5.9 was set again to test reproducibility in interval pH 5.9.

	pH 5.9	pH 5.7	pH 5.5	pH 5.9
pH	5.9	5.7	5.5	5.9
$\dot{V}_{G,n}$ / mL.min ⁻¹		← 111 →		126
H ₂ /CO/CO ₂ /N ₂ / vol. %		← 65.5/18/7/10.5 →		66/18/7/9
H ₂ : CO : CO ₂ / %			← 72:20:8 →	
p / barg			← 0 →	
duration of interval/ h	38	102	78	91
number of gas samples	164	235	329	435
number of liquid samples	4	5	4	4

3. Results and discussion

3.1. Influence of pressure increase at a constant volumetric hydrogen input

Fig. 2 shows the gas uptake rates r , space-time yields STY , and cell density β_{CDW} over the time t of the experiment to investigate the effect of an increased process pressure at a volume-constant hydrogen supply. The experiment is started at ambient pressure conditions (0 barg) and the pressure is subsequently increased in 1 bar increments. After each pressure increase, the establishment of a steady-state condition is waited for, after which the next pressure increase takes place. The evaluation of the steady-state conditions is shown separately in Fig. 3. All measurement data and averaged data of steady-state intervals can be found in supplementary materials.

After increasing the pressure from 0 barg to 1 barg, all three gas uptake rates as well as the cell density and the space-time yield for ethanol initially increase. The gas conversion of CO₂ increases to 93%. To avoid limitation in CO₂ feed, the gas feed of CO₂ is gradually increased by 10% at hour 889, 971, 1010 and 1057, respectively. Immediately after the last increase of CO₂ in the substrate gas, at hour 1058, the gas uptake rates and space-time yields for ethanol reach a local maximum. The space-time yield for ethanol of approximately 10 mmol L⁻¹ h⁻¹ corresponds to a product concentration of 15.33 g L⁻¹. From this point on, the gas uptake rates for CO, CO₂ and H₂ as well as the space-time yield for ethanol decrease continuously until a steady-state condition is reached at hour 729. After increasing the pressure to 2 barg, the gas uptake rates drop again until steady-state, likewise at 3 barg. At 4 barg, the gas uptake rate of H₂ decreases significantly after a short temporary increase, and the cell density also decreases, so that no steady-state conditions are reached. Overall, an inverse behavior of the space-time yields can be seen from hour 1000: while ethanol continuously decreases, the space-time yield for acetic acid continuously increases up to the pressure increase to 4 barg. In addition, it can be seen in Fig. 2 that after pressure increase to 2 barg, 3 barg and 4 barg, the gas uptake rate of CO₂ decreases with a time lag. Furthermore, after each pressure increase, the hydrogen uptake rate temporarily increases before continuously decreasing. This is most visible with the pressure increase to 4 barg at hour 1800 onwards.

The measured data averaged in the steady-state intervals from Fig. 2 on the influence of an increased process pressure with constant-volume hydrogen feed are shown in Fig. 3. The carbon and electron balances range from 88% to 99%.

At ambient pressure (interval 0 barg), the cell density is 3.60 g L⁻¹ (Fig. 3 E) and the product ratio is 1.50 (Fig. 3 F). The space-time yield for acetic acid is consequently 50% higher than that of ethanol (Fig. 3 D). The space-time yield of the C₂ products is 11.21 mmol L⁻¹ h⁻¹, and the biomass-specific productivity of the C₂ products is 3.11 mmol g⁻¹ h⁻¹

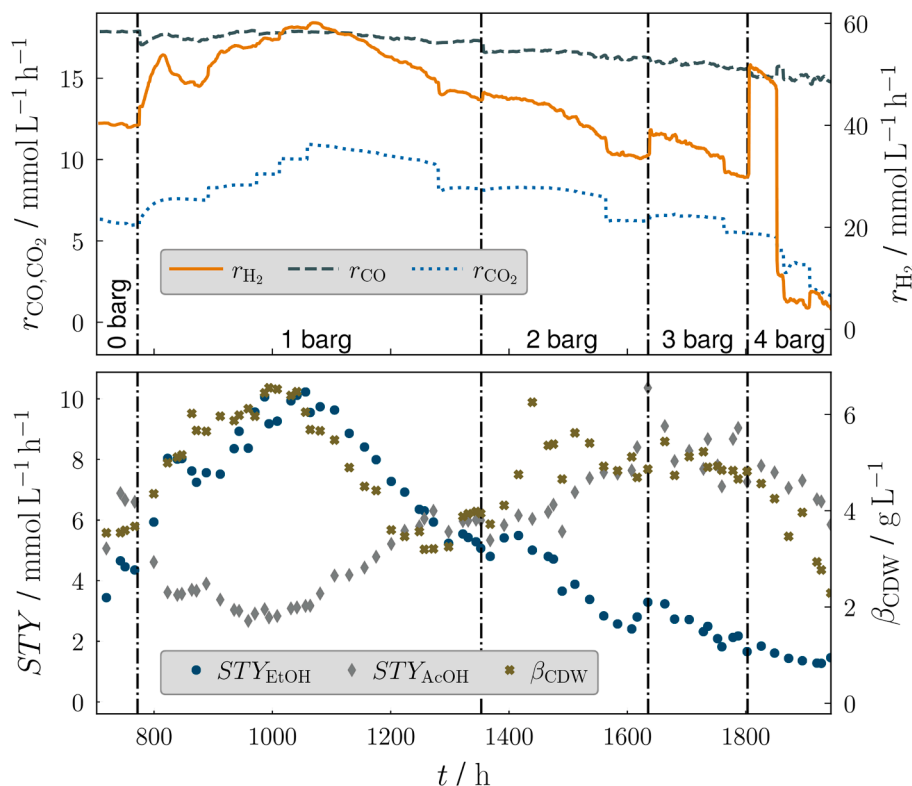


Fig. 2. Measurement data on gas uptake rate r , space-time yield STY and cell density β_{CDW} plotted over the time t of experiment A to investigate the influence of pressure increase with a constant-volume hydrogen supply. The pressure was increased from 0 barg in 1 bar increments to 4 barg. During the periods 729–768 h, 836–878 h, 1293–1353 h, 1575–1630 h and 1765–1803 h, steady-state conditions were established for the pressures 0 barg, 1 barg, 1 barg (at increased CO_2 gas flow), 2 barg and 3 barg. The measured data averaged over these intervals are shown in Fig. 3. At a pressure of 4 barg, no steady-state condition was established.

(Fig. 3 C). In addition to hydrogen, both carbon monoxide and carbon dioxide are taken up by the bacteria. The ratios of the uptaken hydrogen to CO and CO_2 are 2.2 and 6.6, respectively.

The first increase of the process pressure to 1 barg leads to an increase of the cell density by 53% (Fig. 3 E). At the same time, biomass-specific gas uptake decreases for all three substrate gases (Fig. 3 A), this leads to a decreased biomass-specific C_2 productivity (Fig. 3 C). The biomass-specific productivity for acetic acid drops by 64%, while the biomass-specific productivity for ethanol increases slightly by 13%. Therefore, the pressure increase to 1 barg leads to a reduction of the product ratio from initially 1.5 to 0.47 (Fig. 3 F) and consequently results in a higher space-time yield for ethanol compared to acetic acid (Fig. 3 D). The space-time yield of the C_2 products is not affected by the pressure increase to 1 barg.

In order to achieve a volume-constant hydrogen feed, the mass flow rate of hydrogen fed was doubled when the pressure was increased to 1 barg. The gas uptake rate for hydrogen increased with the pressure increase from initially $40 \text{ mmol L}^{-1} \text{ h}^{-1}$ to $48.48 \text{ mmol L}^{-1} \text{ h}^{-1}$, corresponding to an increase of 21% (Fig. 3 B). In comparison to the supplied hydrogen feed, the gas uptake rate thus did not double, so that the conversion of hydrogen dropped from 62% originally to 38%. The conversion of CO_2 has increased from originally 75% to 93%, CO_2 is therefore almost completely taken up after the first pressure increase. In order to avoid a limitation in the availability of CO_2 during further pressure increases, the supplied volume flow of CO_2 is now increased by 21% from initially 6.72 ml min^{-1} to 8.13 ml min^{-1} in an intermediate step, see interval 1 barg($CO_{2,1}$).

Increasing the supplied gas rate of CO_2 leads to a significant decrease in cell density by 30%, see interval 1 barg($CO_{2,1}$) in Fig. 3 E. The conversion of CO_2 decreases from 93% to 85%, the other gas conversions remain almost unchanged. The biomass-specific gas uptake increases for all three substrate gases (Fig. 3 A). The space-time yield of

the C_2 products remains unchanged (-1%), while the space-time yield for acetic acid increases by 63% and decreases by 31% for ethanol (Fig. 3 D). This reverses the product ratio again: from originally 0.47 in the interval 1 barg to 1.11 in the interval 1 barg($CO_{2,1}$) (Fig. 3 F).

As it was already the case for the first pressure increase, the second process pressure increase from 1 barg to 2 barg leads to an increase in cell density, too, the increase is 28% (Fig. 3 E). The biomass-specific gas uptake decreases for all three gases, the reduction is largest for hydrogen with -42% compared to CO_2 with -40% and CO with -26% (Fig. 3 A). The conversion of hydrogen drops from 36% to 18%. There is a further increase in the space-time yield of acetic acid, while the space-time yield of ethanol decreases again (Fig. 3 D). This increases the product ratio from 1.11 to 3.03 (Fig. 3 F). Furthermore, there is a 7% decrease in the space-time yield of the C_2 products for the first time.

The third and last pressure increase in Fig. 3 from 2 barg to 3 barg, unlike the previous pressure increases, does not lead to a significant decrease in cell density. The 2% reduction in cell density is within the standard deviation and therefore negligible. Gas conversions continue to drop, with the largest decrease for hydrogen at 33% from 18 to 12 percentage points. There is a further increase in the space-time yield for acetic acid, while the space-time yield for ethanol assumes the lowest value of $1.99 \text{ mmol L}^{-1} \text{ h}^{-1}$ in this series of measurements (Fig. 3 D). The product ratio increases to 4.18 (Fig. 3 F), which is the highest product ratio measured in this series of measurements. The ratio of uptaken hydrogen to CO and CO_2 is 1.9 and 5.5, respectively, which is lower than the ratio of 2.2 and 6.6 before the first pressure increase was applied.

3.2. Influence of a reduced pH value at high cell densities

The measured data on the influence of a reduced pH are shown in Fig. 4. The carbon and electron balances are between 89% and 99%. All

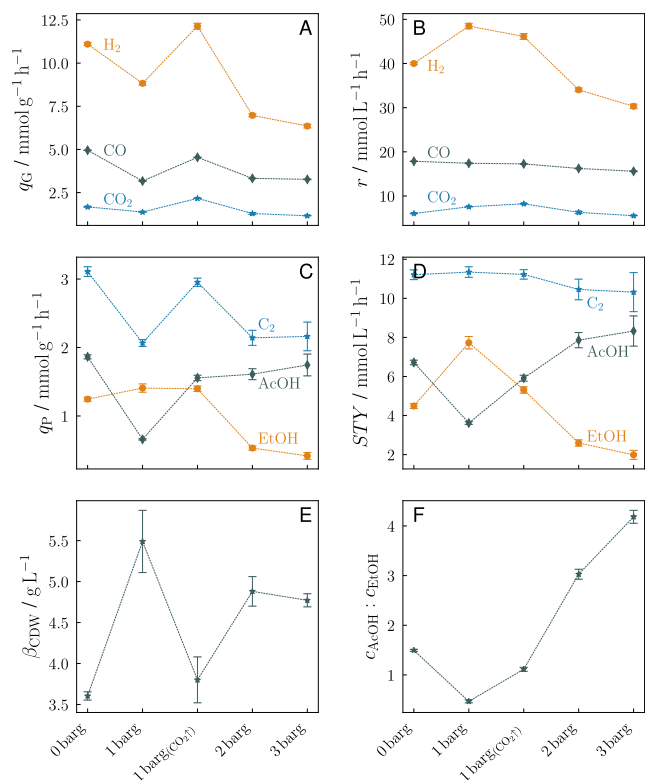


Fig. 3. Influence of a gradual pressure increase to 3 bar gauge pressure with a constant volumetric supply of hydrogen on biomass-specific gas uptake rate q_G (A), gas uptake rate r (B), biomass-specific productivity q_P (C), space-time yield STY (D), mass concentration of biomass β_{CDW} (E), and product ratio of acetic acid to ethanol (F). Averaged measured data of steady-state areas. At one bar overpressure, the amount of CO_2 in the substrate gas was increased in a second step (1 barg(CO_2)). For further details on experimental parameters, see Table 1.

measurement data and averaged data of steady-state intervals can be found in [supplementary materials](#).

The study on the influence of a reduced pH was first started at a pH of 5.9 (pH 5.9), subsequently the pH was reduced to 5.7 (pH 5.7), 5.5 (pH 5.5), 5.3 (pH 5.3) and 5.1 (pH 5.1) and then increased again to 5.9 (pH 5.9).

The first reduction of pH from 5.9 to 5.7 leads to a slight increase in cell density of 8% (Fig. 4 E). The gas uptake rate of hydrogen also increases slightly by 5% (Fig. 4 B). Furthermore, an opposite behavior can be seen in the product formation: while the product formation increases for ethanol, it decreases for acetic acid (Fig. 4 C and D). As a result, the product ratio decreases from 0.8 to 0.62 (Fig. 4 F). The space-time yield of C_2 products increases by 8% along with the pH reduction, and the biomass-specific C_2 product formation remains constant.

Further reduction of pH from 5.7 to 5.5 again leads to a moderate increase in cell density of 7% (Fig. 4 E). For all three gases, the biomass-specific gas uptake rate decreases, by 9% for CO, by 14% for CO_2 and by 15% for hydrogen (Fig. 4 A). Therefore, for the first time, there is also a 13% decrease in biomass-specific C_2 product formation (Fig. 4 C). Furthermore, ethanol productivity decreases in both mass and volume quantities, while acetic acid productivity increases for both benchmarks. Consequently, the product ratio of acetic acid to ethanol increases from 0.62 to 0.9 (Fig. 4 F).

A further reduction of the pH to 5.3 leads to a decreasing gas uptake rate, especially for hydrogen, see Fig. 5. Additionally, after reducing the pH to 5.1, the gas uptake rate of CO_2 decreases significantly. The space-time yield for ethanol decreases from the original $8 \text{ mmol L}^{-1} \text{ h}^{-1}$ at hour 1390 to $2 \text{ mmol L}^{-1} \text{ h}^{-1}$ at hour 1580. With the exception of cell

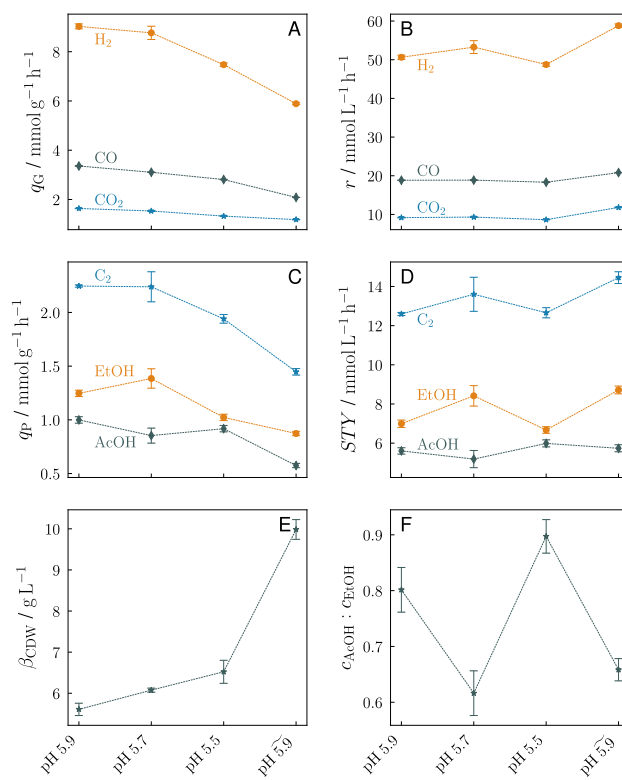


Fig. 4. Influence of a reduced pH value at high cell densities on biomass-specific gas uptake rate q_G (A), gas uptake rate r (B), biomass-specific productivity q_P (C), space-time yield STY (D), mass concentration of biomass β_{CDW} (E), and product ratio of acetic acid to ethanol (F). At the end of the experiment, the pH value of 5.9 investigated at the beginning in interval pH 5.9 was set again to test reproducibility in interval pH 5.9. Averaged measured data of steady-state areas. For further details on experimental parameters, see Table 2.

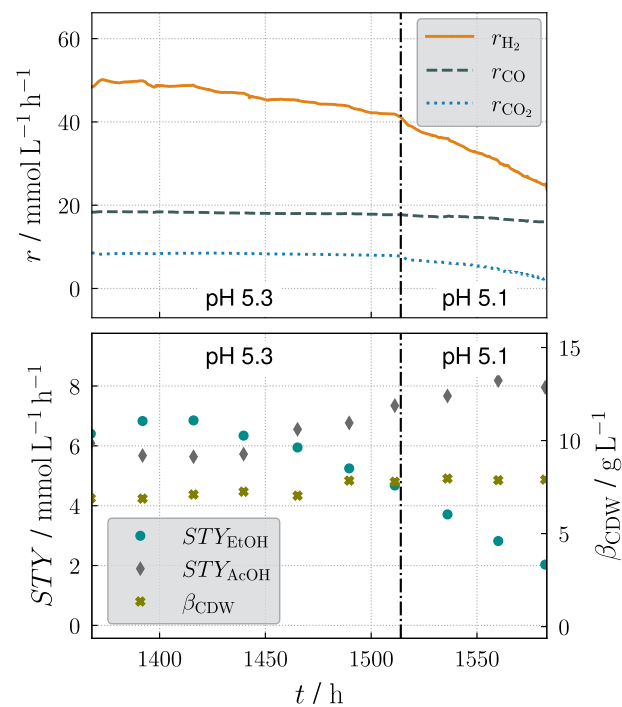


Fig. 5. Non-averaged measured data of gas uptake rates r , space-time yields STY and cell density β_{CDW} over time t for pH 5.3 and 5.1.

density, no steady-state conditions are established, so the measured data at pH 5.3 and 5.1 cannot be averaged and therefore cannot be considered for further evaluation of steady-state intervals.

In a final step, the pH is set to the initial value of 5.9, see interval pH 5.9. In order to have similar gas conversions in the interval pH 5.9 as in the interval pH 5.9, the gas volume flow rate was adjusted and increased in parallel with the increase of pH while keeping the gas composition constant.

The cell density increases significantly with 53% after increasing the pH to 5.9 compared to the interval pH 5.5 (Fig. 4 E). At the same time, the biomass-specific gas uptake rate decreases for all three substrate gases (Fig. 4 A). However, due to the high increase in cell density, there is an overall increase in the gas uptake rate for CO, CO₂ and H₂ (Fig. 4 B). The biomass-specific product formation of ethanol and acetic acid decreases by 15% and 38%, respectively, but the increase in cell density by 53% results in only a slight decrease in the space–time yield of acetic acid of 4% and an increase in the space–time yield of ethanol of 31%. As a result, the fraction of ethanol in the product flow increases, so that the product ratio of acetic acid to ethanol decreases from 0.9 to 0.66 (Fig. 4 F). The space–time yields of ethanol with 8.71 mmol L⁻¹ h⁻¹ and of the C₂ products with 14.45 mmol L⁻¹ h⁻¹ in the interval pH 5.9 are the highest measured space–time yields compared to the other intervals and higher than in the pH 5.9 interval by 25% and 15%, respectively. The space–time yield of ethanol with 8.71 mmol L⁻¹ h⁻¹ corresponds to a product concentration of 13.36 g L⁻¹.

In both experiments, the increase in pressure at a constant volumetric hydrogen input and the lowering of the pH value in the reaction medium were aimed at shifting the product ratio in favor of ethanol. The increase in pressure with constant-volume hydrogen supply was intended to increase hydrogen uptake, while the pH reduction was intended to increase ethanol formation by the cells in order to counteract a further drop in pH. Therefore, the experimental results for pressure increase and pH decrease are discussed below.

3.3. A moderate increase in H₂ partial pressure enhances hydrogen uptake

Only a moderate pressure increase to 1 barg with a constant-volume

hydrogen supply led to an increased hydrogen uptake rate and increased ethanol formation. A further pressure increase to 2 barg and 3 barg resulted in a significantly reduced hydrogen uptake and reduced ethanol formation compared to atmospheric pressure conditions. It can be ruled out that there was too low a concentration of hydrogen in the reaction medium responsible for this development, since the theoretical equilibrium concentration of hydrogen in the liquid phase increased with pressure increase at constant-volume hydrogen feed. The theoretical equilibrium concentration of hydrogen in the liquid phase c_{1,H_2}^* is calculated as follows (Stoll, 2021):

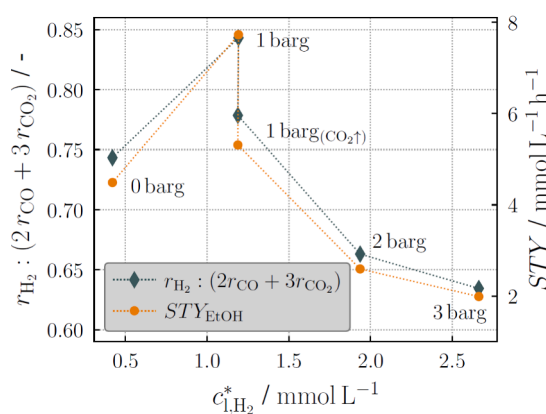
$$c_{1,H_2}^* = y_{H_2} \cdot p_R \cdot H_{H_2} \quad (2)$$

y_{H_2} represents the mole fraction of hydrogen in the gas phase in the reactor head, p_R the process pressure in the reactor, and H_{H_2} the Henry's law constant. For 37 °C, there is a value for H_{H_2} of 0.72 mol m⁻³ bar⁻¹ (Stoll, 2021). Fig. 6a shows the ratio of the hydrogen uptake rate to the carbon uptake rate and the space–time yield of ethanol as a function of the calculated theoretical equilibrium concentration of hydrogen in the liquid phase.

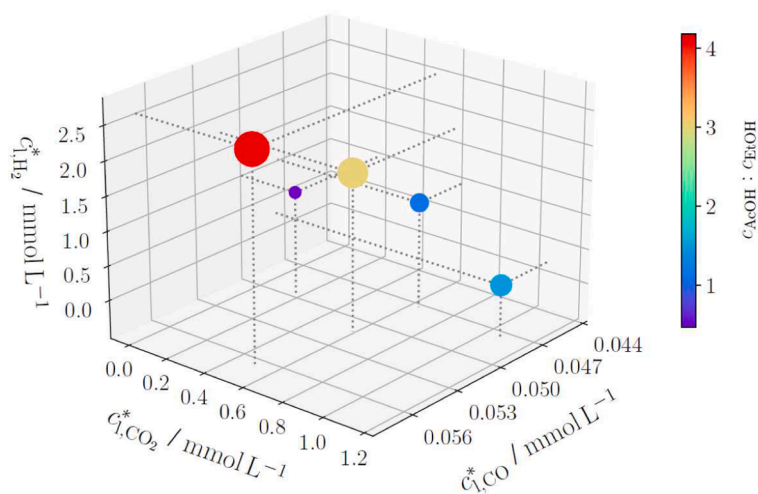
It can be clearly seen that at an equilibrium concentration of $c_{1,H_2}^* = 1.2$ mmol L⁻¹ the ratio of the hydrogen uptake rate to the carbon uptake rate becomes maximum and drops sharply at higher concentrations. The plot of the space–time yield of ethanol shows great agreement with the plot of the ratio of hydrogen uptake rate to carbon uptake rate; similarly, the maximum space–time yield of ethanol is at an equilibrium concentration c_{1,H_2}^* of 1.2 mmol L⁻¹. Fig. 6a therefore suggests that above a critical equilibrium concentration of hydrogen in the liquid phase of 1.2 mmol L⁻¹, an enzymatic reaction is inhibited. This might be the reason for the reduced ethanol formation, as seen in Fig. 6a.

Fig. 6b shows the influence of the theoretical equilibrium concentrations in the liquid phase c_{1,H_2}^* , $c_{1,CO}^* = y_{CO} \cdot p_R \cdot H_{CO}$, and $c_{1,CO_2}^* = y_{CO_2} \cdot p_R \cdot H_{CO_2}$ for all three substrate gases on the product ratio of acetic acid to ethanol.

Similarly, the product ratio of acetic acid to ethanol is smallest at a theoretical equilibrium concentration of hydrogen in the liquid phase of 1.2 mmol L⁻¹, see Fig. 6b. Moreover, it is clear that the concentration of CO₂ in the liquid phase has no significant influence on the product



(a)



(b)

Fig. 6. Influence of theoretical equilibrium concentrations of gases in the liquid phase on gas uptake rates, space–time yields, and product ratios. Gas uptake ratio of hydrogen to carbon and space–time yield of ethanol as a function of c_{1,H_2}^* (a), the gas uptake ratio of hydrogen to carbon takes into account that twice the molar amount of hydrogen is required for the complete conversion of CO to ethanol and three times the molar amount of hydrogen is required for the complete conversion of CO₂ to ethanol. Molar product ratio of acetic acid to ethanol as a function of c_{1,H_2}^* , $c_{1,CO}^*$ and c_{1,CO_2}^* (b), the size of the circle is proportional to the product ratio.

ratio, no dependency between the product ratio and the CO₂ concentration can be seen. In contrast, for the theoretical equilibrium concentration of CO and the product ratio, there is a trend for the product ratio to be low at equilibrium concentrations of 0.052 mmolL⁻¹ and smaller, while high product ratios are present at equilibrium concentrations greater than 0.052 mmolL⁻¹. A clear relationship between hydrogen uptake, product ratio, and biomass-specific partial pressure of CO in the exhaust gas has already been shown in Perret et al. (2023). Therefore, there are two novel findings from Fig. 6a and Fig. 6b:

1. Above a theoretical equilibrium concentration of hydrogen in the liquid phase of $c_{i,H_2}^* = 1.2 \text{ mmolL}^{-1}$, hydrogen uptake is inhibited.
2. The theoretical equilibrium concentration of CO₂ in the liquid phase has been shown to have no effect on the product ratio in the studied range of $c_{i,CO_2}^* = 0.3 \dots 1.2 \text{ mmolL}^{-1}$.

3.3.1. Inhibition of hydrogen uptake

To achieve the above equilibrium concentration of hydrogen in the liquid phase of 1.2 mmolL⁻¹, an elevated process pressure is necessary. Since at atmospheric pressure conditions and a mole fraction of hydrogen in the gas phase in the reactor head to a maximum value of 1, a theoretical equilibrium concentration according to Eq. 2 of maximum 0.72 mmolL⁻¹ would be possible. However, according to Häusler et al. (2016) it is unlikely that the process pressure itself has such an influence on the bacteria, it is rather the concentrations of reactants and products in the liquid phase that have a crucial influence on the bacteria. In their studies with a STR and *C. ljungdahliae* at $c_{i,H_2}^* = 1.91 \text{ mmolL}^{-1}$, Oswald et al. (2018) have detected a significant decrease in ethanol and acetic acid and a significant increase in the less reduced product formic acid compared to $c_{i,H_2}^* = 0.48 \text{ mmolL}^{-1}$. Results of Stoll et al. (2019) also show a decrease in ethanol productivity and an increase in acetic and formic acid productivity upon increasing c_{i,H_2}^* from 0.36 mmolL⁻¹ to 1.47 mmolL⁻¹ with the same organism in a STR. These results confirm the observation of inhibition above $c_{i,H_2}^* = 1.2 \text{ mmolL}^{-1}$ in the present study.

Despite the reduced hydrogen uptake at increased theoretical equilibrium concentrations of H₂, the space–time yield of the C₂ products dropped only slightly, from 11.35 mmolL⁻¹h⁻¹ at 1 barg by 9% to 10.32 mmolL⁻¹h⁻¹ at 3 barg, while the hydrogen uptake rate r_{H_2} dropped by 37%. In contrast to CO inhibition, which significantly reduces C₂ productivity and cell density, see Perret et al. (2023), a high hydrogen concentration in the liquid phase appears to significantly inhibit hydrogen uptake but not the other processes in metabolism. Therefore, at approximately constant C₂ productivity, there is only a shift in the product ratio towards acetic acid.

3.3.2. No inhibitory effect by CO₂

Eigenstetter and Takors (2017) have found in studies with the yeast *Saccharomyces cerevisiae* that high CO₂ concentrations in the liquid phase increase the ATP requirement to maintain cell metabolism in the long term. In terms of syngas fermentation, this would mean that increased energy requirements for metabolism would result in the formation of fewer reduced products such as ethanol, and that the product ratio of acetic acid to ethanol would increase. However, Fig. 6b does not show that as the theoretical equilibrium concentration of CO₂ in the liquid phase increases in the range of 0.3...1.2 mmolL⁻¹, the product ratio increases.

3.3.3. High ethanol concentrations are not sustainable over the long-term

In Fig. 2 over the period 750h–1300h, acetic acid productivity initially starts to fall to a minimum of about 3 mmolL⁻¹h⁻¹ and then rises again to a value of 6 mmolL⁻¹h⁻¹. Ethanol productivity behaves in

the opposite direction, first increasing to a maximum of 10 mmolL⁻¹h⁻¹ and then decreasing to 5.5 mmolL⁻¹h⁻¹. The space–time yield of 10 mmolL⁻¹h⁻¹ for ethanol, corresponding to a product concentration of 15.36 gL⁻¹, is the highest space–time yield measured to date with the wild type of *C. ljungdahliae*. It is even higher by 15% when compared to Perret et al. (2023), who claim the highest measured space–time yield to date. However, it can be seen in Fig. 2 that this high space–time yield of ethanol is obviously not stable over time. It is possible that this might be the result of inhibition by the high ethanol concentration due to the chaotropic characteristic of ethanol (Valgepea et al., 2017). This would also explain the decrease in cell density. Ramió-Pujol et al. (2018) did not observe any inhibitory effect in their studies with *C. ljungdahliae* at ethanol concentrations lower than 15 gL⁻¹. The product concentration of 15.36 gL⁻¹ in the present experiment is slightly above the study range of Ramió-Pujol et al. (2018), so inhibition at this concentration cannot be ruled out. However, Phillips et al. (1993) achieved even higher ethanol concentrations of up to 48 gL⁻¹ in continuous fermentation experiments with *C. ljungdahliae*, so inhibition by ethanol at concentrations as high as 15.36 gL⁻¹ is unlikely.

Another possible cause for the drop in ethanol productivity starting at time 1060h could be an imbalance in cell metabolism and a decrease in AcetylCoA pool, a finding made by Valgepea et al. (2017). Due to ethanol productivity and the associated need for reduction potential, there would be a decrease in AcetylCoA pool and cell density due to a lagging WLP. This would explain the decrease in ethanol productivity and increase in acetic acid formation, as the reduced need for reduction potential to synthesize acetic acid compared to ethanol would restore the balance in cell metabolism.

3.4. pH lower than 5.7 leads to increased acetic acid formation

When the pH was reduced starting from 5.9 to 5.7, 5.5, 5.3, and 5.1, a lower acetic acid to ethanol ratio of 0.62 was observed only at pH 5.7 compared to 0.8 at pH 5.9, see Figs. 4 and 5. At lower pH values, the ratio even increases and reaches a value of 4 in the non-steady state region of pH 5.1.

In contrast, Mohammadi et al. (2012) observed in their studies with *C. ljungdahliae* in a CSTR without cell retention an increase in ethanol concentration and a decrease in acetic acid concentration upon reduction of a non-regulated pH. This resulted in a reduction in the acetic acid to ethanol product ratio from initially 1.38 to 0.31. However, their measured space–time yields for ethanol and acetic acid of 1.79 mmolL⁻¹h⁻¹ and 0.55 mmolL⁻¹h⁻¹, respectively, are significantly lower than the space–time yields obtained in the present investigation of pH reduction. Abubackar et al. (2015) have been able to significantly reduce the acetic acid to ethanol product ratio with a similar organism, *C. autoethanogenum*, in STR by lowering the pH from 6 to 4.75, since at pH 4.75 the acetic acid concentration dropped from previously 900 mgL⁻¹ to below 50 mgL⁻¹ with an almost constant ethanol concentration. Also, in another study of cyclic lowering and raising of pH, Abubackar et al. (2016) found a significant reduction in the product ratio of acetic acid to ethanol at lower pH values. However, in both studies, cell densities with concentrations of 0.3 gL⁻¹ at maximum were significantly lower than in the present study with total cell retention and cell densities of up to 10 gL⁻¹. On the other hand, Infantes et al. (2020) observed in their studies with *C. ljungdahliae* in a STR a nearly constant acetic acid to ethanol product ratio of 11.69 compared to 11.49 when the pH was reduced from 5.9 to 5.4. In a study using non-growing cells of *C. ljungdahliae*, Cotter et al. (2009) found that lowering pH did not increase ethanol productivity and attributed this to reduced proton pump activity in non-growing cells (Cotter and Hill, 2003).

The results of the above analyses show that a reduction in pH does not necessarily lead to a lower product ratio of acetic acid to ethanol. In the present study with total cell retention and constant cell density in

steady-state areas, it is likely that the growth of cells is very low and just enough to compensate for the isolated death of cells. It is therefore possible that the activity of the proton pumps of these cells is, in analogy to the non-growing cells at Cotter et al. (2009), greatly reduced and therefore, despite reduction of pH to values below 5.7, there is no further decrease in the product ratio. At pH values of 5.3 and 5.1, gas uptake and ethanol productivity decrease steadily, and no steady-state is established. Cell density, on the other hand, remains constant, this could be an indicator that although the cells do not die, viability decreases. This is supported by studies by Cotter et al. (2009), showing that at a pH of 5.5, viability is only 44%, and at a pH of 4.5, viability is only 11%.

The re-raising of pH to the initial value of 5.9 in this experimental run and the renewed increase in ethanol productivity and C₂ productivity overall indicate that the cells have recovered from the unfavorable growth conditions at low pH values. However, the increase in cell density to 9.98 g L⁻¹ and the decrease in biomass-specific productivity indicate that a certain amount of cells continue to have low or no viability, but these cells have nevertheless not died. However, it would also be possible, analogous to the studies of Kwon et al. (2022), that the cells have metabolically changed during the 1600 process hours due to lowering pH and due to increased acetic acid concentrations up to 16 g L⁻¹. Increased cell density, higher space–time yield of ethanol, and at the same time lower biomass-specific productivity were reported by Kwon et al. (2022) and also found to be true for the measured results in the present study. Thus, the increased space–time yield of ethanol with 8.71 mmol L⁻¹ h⁻¹ after raising the pH to 5.9 compared to 6.99 mmol L⁻¹ h⁻¹ at the beginning of the experimental series at pH 5.9 could be attributed to mutational processes. However, the number of cell generations over a 1600 h run time is low when total cell retention is used: assuming that cells do not die and therefore do not have to be regenerated and assuming a dilution rate of 0.00244 h⁻¹ due to daily sampling, the doubling time is 415.99 h and the number of cell generations over a 1600 h run time is thus at least 4. In fact, due to dying cells, among others, this number will be higher, but at most 49. This would correspond to operation without cell retention and assuming a growth rate of $\mu = D = 0.03 \text{ h}^{-1}$. The focus of the present study is to obtain kinetic data and to determine the fundamentals of reaction engineering. However, further studies, in particular mutational genes analysis, are needed to determine to what extent the increased space–time yield of ethanol can really be attributed to mutational processes.

4. Conclusions

An increase in the hydrogen partial pressure to 1.52 bar enhances hydrogen uptake and space–time yield of ethanol, and the product ratio can thus be shifted in the direction of ethanol. However, the measured data clearly show that above a partial pressure of hydrogen of 1.52 bar, corresponding to a theoretical equilibrium concentration of $c_{\text{H}_2}^* = 1.2 \text{ mmol L}^{-1}$, hydrogen uptake decreases significantly. In addition, a moderate reduction of the pH from 5.9 to 5.7 leads to increased hydrogen uptake and a shift of the product ratio towards ethanol. A further decrease in pH reduces hydrogen uptake and ethanol productivity.

CRediT authorship contribution statement

Lukas Perret: Conceptualization, Methodology, Investigation, Validation, Formal analysis, Funding acquisition, Visualization, Writing - original draft. **Nikolaos Boukis:** Conceptualization, Funding acquisition, Writing - review & editing. **Jörg Sauer:** Conceptualization, Supervision, Project administration, Funding acquisition, Writing - review & editing.

Declaration of Competing Interest

The authors declare that they have no known competing financial interests or personal relationships that could have appeared to influence the work reported in this paper.

Data availability

Datasets related to this article can be found at <https://doi.org/10.17632/nnx6brc9hj.1>, an open-source online data repository hosted at Mendeley Data (Perret et al., 2023).

Acknowledgements

The authors thank the Federal Ministry of Education and Research (BMBF) for financing the R&D program (Grant No. 03SFK2K0-2). We also gratefully acknowledge the funding of the Helmholtz Research Program “Materials and Technologies for the Energy Transition (MTET), Topic 3: Chemical Energy Carriers”. The authors would also like to thank E. Hauer for the contributions to the experimental work, K. Weiss and S. Henecka for the contributions to the mechanical work and V. Holderied and A. Lautenbach for the contributions to the analytical measurement.

Appendix A. Supplementary data

Supplementary data associated with this article can be found, in the online version, at <https://doi.org/10.1016/j.biortech.2023.129894>.

References

- Abubackar, H.N., Fernández-Naveira, Á., Veiga, M.C., Kennes, C., 2016. Impact of cyclic pH shifts on carbon monoxide fermentation to ethanol by clostridium autoethanogenum. *Fuel* 178, 56–62. <https://doi.org/10.1016/j.fuel.2016.03.048>.
- Abubackar, H.N., Veiga, M.C., Kennes, C., 2015. Carbon monoxide fermentation to ethanol by clostridium autoethanogenum in a bioreactor with no accumulation of acetic acid. *Bioresour. Technol.* 186, 122–127. <https://doi.org/10.1016/j.biortech.2015.02.113>.
- Abubackar, H.N., Veiga, M.C., Kennes, C., 2018. Production of acids and alcohols from syngas in a two-stage continuous fermentation process. *Bioresour. Technol.* 253, 227–234. <https://doi.org/10.1016/j.biortech.2018.01.026>.
- Cotter, J.L., Chinn, M.S., Grunden, A.M., 2009. Ethanol and acetate production by clostridium ljungdahlii and clostridium autoethanogenum using resting cells. *Bioprocess. Biosyst. Eng.* 32, 369–380. <https://doi.org/10.1007/s00449-008-0256-y>.
- Cotter, P.D., Hill, C., 2003. Surviving the acid test: responses of gram-positive bacteria to low pH. *Microbiol. Mol. Biol. Rev.* 67, 429–53, table of contents. doi: 10.1128/MMBR.67.3.429-453.2003.
- Eigenstetter, G., Takors, R., 2017. Dynamic modeling reveals a three-step response of saccharomyces cerevisiae to high co2 levels accompanied by increasing atp demands. *FEMS Yeast Res.* 17 <https://doi.org/10.1093/femsyr/fox008>.
- Fernández-Blanco, C., Robles-Iglesias, R., Naveira-Pazos, C., Veiga, M.C., Kennes, C., 2023. Production of biofuels from c1 -gases with clostridium and related bacteria-recent advances. *Microb. Biotechnol.* 16, 726–741. <https://doi.org/10.1111/1751-7915.14220>.
- Häusler, E.B.G., van der Wielen, L.A.M., Straathof, A.J.J., 2016. Evaluation of gas supply configurations for microbial product formation involving multiple gaseous substrates. *Bioresour. Bioprocess.* 3, 868. <https://doi.org/10.1186/s40643-016-0095-7>.
- Infantes, A., Kugel, M., Neumann, A., 2020. Evaluation of media components and process parameters in a sensitive and robust fed-batch syngas fermentation system with clostridium ljungdahlii. *Fermentation* 6, 61. <https://doi.org/10.3390/fermentation6020061>.
- Kwon, S.J., Lee, J., Lee, H.S., 2022. Metabolic changes of the acetogen clostridium sp. awrp through adaptation to acetate challenge. *Front. Microbiol.* 13, 982442 <https://doi.org/10.3389/fmicb.2022.982442>.
- Mohammadi, M., Younesi, H., Najafpour, G., Mohamed, A.R., 2012. Sustainable ethanol fermentation from synthesis gas by clostridium ljungdahlii in a continuous stirred tank bioreactor. *J. Chem. Technol. Biotechnol.* 87, 837–843. <https://doi.org/10.1002/jctb.3712>.
- Oswald, F., Zwick, M., Omar, O., Hotz, E.N., Neumann, A., 2018. Growth and product formation of clostridium ljungdahlii in presence of cyanide. *Front. Microbiol.* 9, 1213. <https://doi.org/10.3389/fmicb.2018.01213>.
- Perret, L., Boukis, N., Sauer, J., 2023. Influence of increased cell densities on product ratio and productivity in syngas fermentation. *Ind. Eng. Chem. Res.* 62, 13799–13810. <https://doi.org/10.1021/acs.iecr.3c01911>.

- Perret, P., Boukis, N., Sauer, J., 2023. Raw measurement data on the influence of pH and H₂ partial pressure on syngas fermentation with *Clostridium ljungdahlii*. Mendeley Data. <https://doi.org/10.17632/nxx6brc9hj.1>.
- Perret, L., de Oliveira, Lacerda, Campos, B., Herrera Delgado, K., Zevaco, T.A., Neumann, A., Sauer, J., 2022. CO₂ fixation to elementary building blocks: Anaerobic syngas fermentation vs. chemical catalysis. *Chem. Ing. Tech.* 94, 1667–1687. <https://doi.org/10.1002/cite.202200153>.
- Phillips, J.R., Klasson, K.T., Clausen, E.C., Gaddy, J.L., 1993. Biological production of ethanol from coal synthesis gas. *Appl. Biochem. Biotechnol.* 39–40, 559–571. <https://doi.org/10.1007/BF02919018>.
- Ramió-Pujol, S., Ganigué, R., Bañeras, L., Colprim, J., 2018. Effect of ethanol and butanol on autotrophic growth of model homoacetogens. *FEMS Microbiol. Lett.* 365, 1–4. <https://doi.org/10.1093/femsle/fny084>.
- Stoll, I.K., 2021. Influence of increased process pressure during fermentation of synthesis gas: Characterization of pressure fermentation in the stirred tank reactor, Dissertation. Karlsruhe Institute of Technology, Karlsruhe.
- Stoll, I.K., Boukis, N., Sauer, J., 2019. Syngas fermentation at elevated pressure - experimental results, 1255–1261 doi: 10.5071/27theubce2019-3cv.3.4.
- Valgepea, K., de Souza Pinto Lemgruber, R., Meaghan, K., Palfreyman, R.W., Abdalla, T., Heijstra, B.D., Behrendorf, J.B., Tappel, R., Köpke, M., Simpson, S.D., Nielsen, L.K., Marcellin, E., 2017. Maintenance of ATP homeostasis triggers metabolic shifts in gas-fermenting acetogens. *Cell Syst.* 4, 505–515. doi: 10.1016/j.cels.2017.04.008.
- Younesi, H., Najafpour, G., Mohamed, A.R., 2005. Ethanol and acetate production from synthesis gas via fermentation processes using anaerobic bacterium, *Clostridium ljungdahlii*. *Biochem. Eng. J.* 27, 110–119. <https://doi.org/10.1016/j.bej.2005.08.015>.